

Learning Physical-Layer Communication with Quantized Feedback

Jinxiang Song, Bile Peng, Christian Häger, Henk Wymeersch, Anant Sahai

Abstract—Data-driven optimization of transmitters and receivers can reveal new modulation and detection schemes and enable physical-layer communication over unknown channels. Previous work has shown that practical implementations of this approach require a feedback signal from the receiver to the transmitter. In this paper, we study the impact of quantized feedback in data-driven learning of physical-layer communication. A novel quantization method is proposed, which exploits the specific properties of the feedback signal and is suitable for non-stationary signal distributions. The method is evaluated for linear and nonlinear channels. Simulation results show that feedback quantization does not appreciably affect the learning process and can lead to excellent performance, even with 1-bit quantization. In addition, it is shown that learning is surprisingly robust to noisy feedback where random bit flips are applied to the quantization bits.

I. INTRODUCTION

As communication systems become more complex, designing optimal transmission and detection methods has become harder as well. This is true not only in wireless communication, where hardware impairments and quantization have increasingly become a limitation on the achievable performance, but also in optical communication, for which the nonlinear nature of the channel precludes the use of standard approaches. This has led to a new line of research where transmission and detection methods are learned from data. The general idea is to regard the transmitter and receiver as parameterized functions (e.g., neural networks) and find good parameter configurations using large-scale gradient-based optimization approaches from machine learning.

Data-driven methods have mainly focused on learning receivers assuming a given transmitter and channel, e.g., for MIMO detection [1] or decoding [2]. These methods have led to algorithms that either perform better or exhibit lower complexity than model-based algorithms. More recently, end-to-end learning of both the transmitter and receiver has been proposed for various applications including wireless [3], [4], nonlinear optical [5]–[7], and visible light communication [8].

In practice, gradient-based transmitter optimization is problematic since it requires a known and differentiable channel

model. One approach to circumvent this limitation is to first learn a surrogate channel model, e.g., through an adversarial process, and use the surrogate model for the optimization [9], [10]. We follow a different approach based on stochastic transmitters, where the transmitted symbol for a fixed message is assumed to be a random variable during the training process [11]–[13]. This allows for the computation of *surrogate gradients* which can then be used to update the transmitter parameters. A related approach is proposed in [14].¹

In order to compute the surrogate gradients, the transmitter must receive a *feedback signal* from the receiver. This feedback signal can either be perfect [11]–[14] or noisy [15]. In the latter case, it is instructive to regard the feedback transmission as a separate communication problem for which optimized transmitter and receiver pairs can again be learned. This view was taken in [15], where the feedback link allowed for transmission of real numbers over an additive white Gaussian noise (AWGN) channel. In practice, however, signals will be quantized to a finite number of bits, including the feedback signal. To the best of our knowledge, such quantization has not yet been considered in the literature. Studies on quantization have been conducted so far only in terms of the transmitter and receiver processing, for example when the corresponding learned models are implemented with finite resolution [16]–[20].

In this paper, we analyze the impact of quantization of the feedback signal in data-driven learning of physical-layer communication over an unknown channel. We show that due to the specific properties of the feedback signal, an adaptive pre-processing followed by a fixed quantization strategy can lead to excellent performance, even with 1-bit quantization. We provide a theoretical justification for the proposed approach and perform extensive simulations for both linear Gaussian and nonlinear optical channels.

Notation: Vectors will be denoted with lower case letters in bold (e.g., \mathbf{x}), with x_n or $[\mathbf{x}]_n$ referring to the n -th entry in \mathbf{x} ; matrices will be denoted in bold capitals (e.g., \mathbf{X}); $\mathbb{V}(\mathbf{x})$ denotes the variance (the trace of the covariance matrix) of the random vector \mathbf{x} (i.e., $\mathbb{V}\{\mathbf{x}\} = \mathbb{E}\{\mathbf{x}\mathbf{x}^T\} - (\mathbb{E}\{\mathbf{x}\})^T(\mathbb{E}\{\mathbf{x}\})$).

II. SYSTEM MODEL

We wish to transmit messages $m \in \{1, \dots, M\} \triangleq [M]$ over an a priori unknown memoryless channel which is defined by a conditional probability density function (PDF) $p(y|x)$,

¹See [12, Sec. III-C] for a discussion about the relationship between the approaches in [11]–[13] and [14].

J. Song, B. Peng, C. Häger, and H. Wymeersch are with the Department of Electrical Engineering, Chalmers University of Technology, Gothenburg, Sweden. email: jinxiang@student.chalmers.se, {bile.peng, christian.haeger, henkw}@chalmers.se. C. Häger is also with the Department of Electrical and Computer Engineering, Duke University, Durham, USA. A. Sahai is with the Department of Electrical Engineering and Computer Science, UC Berkeley, Berkeley, USA. The work of C. Häger was supported by the European Union's Horizon 2020 research and innovation programme under the Marie Skłodowska-Curie grant No. 749798. H. Wymeersch was supported by the Swedish Research Council under grant No. 2018-03701.

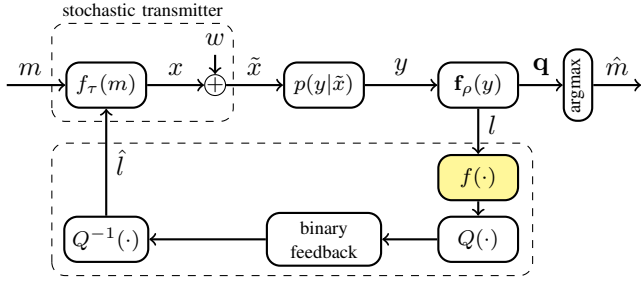


Fig. 1: Data-driven learning model where the discrete time index k (e.g., m_k) is omitted for all variables. The quantization and binary feedback is shown in the lower dashed box, while the proposed pre-processor is highlighted. Note that $w = 0$ for the receiver learning (Sec. III-A).

where $x, y \in \mathbb{C}$ and M is the total number of messages.² The communication system is implemented by representing the transmitter and receiver as two parameterized functions $f_\tau : [M] \rightarrow \mathbb{C}$ and $\mathbf{f}_\rho : \mathbb{C} \rightarrow [0, 1]^M$, where τ and ρ are sets of transmitter and receiver parameters, respectively. The transmitter maps the k -th message m_k to a complex symbol $x_k = f_\tau(m_k)$, where an average power constraint according to $\mathbb{E}\{|x_k|^2\} \leq P$ is assumed. The symbol x_k is sent over the channel and the receiver maps the channel observation y_k to a probability vector $\mathbf{q}_k = \mathbf{f}_\rho(y_k)$, where one may interpret the components of \mathbf{q}_k as estimated posterior probabilities for each possible message. Finally, the receiver outputs an estimated message according to $\hat{m}_k = \arg \max_m [\mathbf{q}_k]_m$, where $[\mathbf{x}]_m$ returns the m -th component of \mathbf{x} . The setup is depicted in the top branch of the block diagram in Fig. 1, where the random perturbation w in the transmitter can be ignored for now.

We further assume that there exists a feedback link from the receiver to the transmitter, which, as we will see below, facilitates transmitter learning. In general, our goal is to learn optimal transmitter and receiver mappings f_τ and \mathbf{f}_ρ using limited feedback.

III. DATA-DRIVEN LEARNING

In order to find good parameter configurations for τ and ρ , a suitable optimization criterion is required. Due to the reliance on gradient-based methods, conventional criteria such as the symbol error probability $\text{Pr}(m_k \neq \hat{m}_k)$ cannot be used directly. Instead, it is common to minimize the expected cross-entropy loss defined by

$$\ell(\tau, \rho) \triangleq -\mathbb{E}\{\log([\mathbf{f}_\rho(y_k)]_{m_k})\}, \quad (1)$$

where the dependence of $\ell(\tau, \rho)$ on τ is implicit through the distribution of y_k .

A major practical hurdle is the fact that the gradient $\nabla_\tau \ell(\tau, \rho)$ cannot actually be evaluated because it requires a known and differentiable channel model. To solve this problem, we apply the alternating optimization approach proposed in [11], [12], which we briefly review in the following. For this approach, one alternates between optimizing first the receiver parameters ρ and then the transmitter parameters τ for a certain

²In this paper, we restrict ourselves to two-dimensional (i.e., complex-valued) channel models, where the generalization to an arbitrary number of dimensions is straightforward.

number of iterations N . To that end, it is assumed that the transmitter and receiver share common knowledge about a database of training data m_k .

A. Receiver Learning

For the receiver optimization, the transmitter parameters τ are assumed to be fixed. The transmitter maps a mini-batch of uniformly random training messages m_k , $k \in [B_R]$, to symbols satisfying the power constraint and transmits them over the channel. The receiver observes y_1, \dots, y_{B_R} and generates B_R probability vectors $\mathbf{f}_\rho(y_1), \dots, \mathbf{f}_\rho(y_{B_R})$. The receiver then updates its parameters ρ according to $\rho_{i+1} = \rho_i - \alpha_R \nabla_\rho \ell_R^e(\rho_i)$, where

$$\ell_R^e(\rho) = -\frac{1}{B_R} \sum_{k=1}^{B_R} \log([\mathbf{f}_\rho(y_k)]_{m_k}) \quad (2)$$

is the empirical cross-entropy loss associated with the mini-batch and α_R is the learning rate. This procedure is repeated iteratively for a fixed number of iterations N_R .

B. Transmitter Learning

For the transmitter optimization, the receiver parameters are assumed to be fixed. The transmitter generates a mini-batch of uniformly random training messages m_k , $k \in [B_T]$, and performs the symbol mapping as before. However, before transmitting the symbols over the channel, a small Gaussian perturbation is applied, which yields $\tilde{x}_k = x_k + w_k$, where $w_k \sim \mathcal{CN}(0, \sigma_p^2)$ and reasonable choices for σ_p^2 are discussed in Sec. V. Hence, we can interpret the transmitter as stochastic, described by the PDF

$$\pi_\tau(\tilde{x}_k | m_k) = \frac{1}{\pi \sigma_p^2} \exp\left(-\frac{|\tilde{x}_k - f_\tau(m_k)|^2}{\sigma_p^2}\right). \quad (3)$$

Based on the received channel observations, the receiver then computes per-sample losses $l_k = -\log([\mathbf{f}_\rho(y_k)]_{m_k}) \in \mathbb{R}$ for $k \in [B_T]$ and feeds these back to the transmitter via the feedback link. The corresponding received losses are denoted by \hat{l}_k , where ideal feedback corresponds to $\hat{l}_k = l_k$. Finally, the transmitter updates its parameters τ according to $\tau_{i+1} = \tau_i - \alpha \nabla_\tau \ell_T^e(\tau_i)$, where

$$\nabla_\tau \ell_T^e(\tau) = \frac{1}{B_T} \sum_{k=1}^{B_T} \hat{l}_k \nabla_\tau \log \pi_\tau(\tilde{x}_k | m_k). \quad (4)$$

This procedure is repeated iteratively for a fixed number of iterations N_T , after which the alternating optimization continues again with the receiver learning. The total number of gradient steps in the entire optimization is given by $N(N_T + N_R)$.

A theoretical justification for the gradient in (4) can be found in [11]–[13]. In particular, it can be shown that the gradient of $\ell_T(\tau) = \mathbb{E}\{l_k\}$ is given by

$$\nabla_\tau \ell_T(\tau) = \mathbb{E}\{l_k \nabla_\tau \log \pi_\tau(\tilde{x}_k | m_k)\}, \quad (5)$$

where the expectations are over the message, transmitter, and channel distributions. Note that (4) is the corresponding sample average for finite mini-batches assuming $\hat{l}_k = l_k$.

Remark 1. As pointed out in previous work, the transmitter optimization can be regarded as a simple form of reinforcement learning. In particular, one may interpret the transmitter as an agent exploring its environment according to a stochastic exploration policy defined by (3) and receiving (negative) rewards in the form of per-sample losses. The state is the message m_k and the transmitted symbol \tilde{x}_k is the corresponding action. The learning setup belongs to the class of *policy gradient methods*, which rely on optimizing parameterized policies using gradient descent. We will make use of the following well-known property of policy gradient learning:³

$$\mathbb{E}\{\nabla_{\tau} \log \pi_{\tau}(\tilde{x}_k|m_k)\} = 0. \quad (6)$$

C. Loss Transformation

The per-sample losses can be transformed through a pre-processing function $f: \mathbb{R} \rightarrow \mathbb{R}$ without adversely affecting the performance. This is known as reward shaping in the context of reinforcement learning [21]. Possible examples for f include:

- **Clipping:** setting $f(l_k) = \min(\beta, l_k)$ is used to deal with large loss variations and stabilize training [22].
- **Baseline:** setting $f(l_k) = l_k - \beta$ is called a constant baseline [23] and is often used to reduce the variance of the Monte Carlo estimate of the stochastic gradient [21].
- **Scaling:** setting $f(l_k) = \beta l_k$ only affects the magnitude of the gradient step, but this can be compensated with methods using adaptive step sizes (including the widely used Adam optimizer [24]). However, aggressive scaling can adversely affect the performance [25], [26].

In summary, training with transformed losses, i.e., assuming $\hat{l}_k = f(l_k)$ in (4), is robust to baselines and scaling, while it often operates well with clipping. Hence, the training success is mainly determined by the relative ordering of the losses (i.e., the distinction between good actions and bad actions).

IV. LEARNING WITH QUANTIZED FEEDBACK

Previous work has mostly relied on ideal feedback, where $\hat{l}_k = l_k$ [11]–[14]. Robustness of learning with respect to additive noise according to $\hat{l}_k = l_k + n_k$, $n_k \sim \mathcal{N}(0, \sigma^2)$, was demonstrated in [15]. In this paper, we take a different view and assume that there only exists a *binary feedback channel* from the receiver to the transmitter. In this case, the losses must be quantized before transmission.

A. Conventional Quantization

Optimal Quantization: Given a distribution of the losses $p(l_k)$ and q bits that can be used for quantization, the mean squared quantization error is

$$D = \mathbb{E}\{(l_k - Q(l_k))^2\}. \quad (7)$$

With q bits, there are 2^q possible quantization levels which can be optimized to minimize D , e.g., using the Lloyd-Max algorithm [27].

³To see this, one may first apply $\nabla_{\tau} \log \pi_{\tau} = \frac{\nabla_{\tau} \pi_{\tau}}{\pi_{\tau}}$ and then use the fact that $\int \nabla_{\tau} \pi_{\tau}(\tilde{x}|m) d\tilde{x} = 0$ since $\int \pi_{\tau}(\tilde{x}|m) d\tilde{x} = 1$.

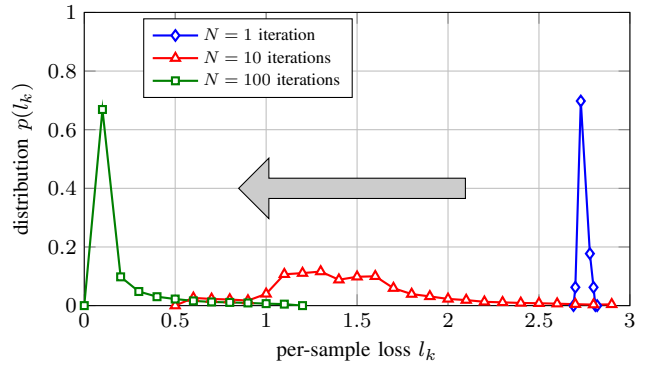


Fig. 2: Illustration of the non-stationary loss distribution as a function of the number of training iterations in the alternating optimization.

Adaptive Quantization: In our setting, the distribution of the per-sample losses varies over time as illustrated in Fig. 2. For non-stationary variables, adaptive quantization can be used. The source distribution can be estimated based on a finite number of previously seen values and then adapted based on the Lloyd-Max algorithm. If the source and sink adapt based on quantized values, no additional information needs to be exchanged. If adaptation is performed based on unquantized samples, the new quantization levels need to be conveyed from source to sink. In either case, a sufficient number of realizations are needed to accurately estimate the loss distribution and the speed of adaptation is fixed.

Fixed Quantization: We aim for a strategy that does not require overhead between transmitter and receiver. A simple non-adaptive strategy is to apply a fixed quantization. Under fixed quantization, we divide up the range $[0, \bar{l}]$ into $2^q - 1$ equal-size regions of size $\Delta = \bar{l}/2^q$ so that $Q(l) = \Delta/2 + \Delta \lfloor l/\Delta \rfloor$. Here, \bar{l} is the largest loss value of interest. Hence, the function $Q(l)$ and its inverse $Q^{-1}(l)$ are fully determined by \bar{l} and the number of bits q .

B. Proposed Quantization

Given the fact that losses can be transformed without much impact on the optimization, as described in Sec. III-C, we propose a novel strategy that employs adaptive pre-processing followed by a fixed quantization scheme. The proposed method operates on mini-batches of size B_T . In particular, the receiver (source) applies the following steps:

- 1) **Clipping:** we clip the losses to lie within a range $[l_{\min}, l_{\max}]$. Here, l_{\min} is the smallest loss in the current mini-batch, while l_{\max} is chosen such that the 5% largest losses in the batch are clipped. This effectively excludes very large per-sample losses which may be regarded as outliers. We denote this operation by $f_{\text{clip}}(\cdot)$.
- 2) **Baseline:** we then shift the losses with a fixed baseline l_{\min} . This ensures that all losses are within the range $[0, l_{\max} - l_{\min}]$. We denote this operation by $f_{\text{bl}}(\cdot)$.
- 3) **Scaling:** we scale all the losses by $1/(l_{\max} - l_{\min})$, so that they are within the range $[0, 1]$. We denote this operation by $f_{\text{sc}}(\cdot)$.
- 4) **Fixed quantization:** finally, we use a fixed quantization with q bits and send $Q(\tilde{l}_k)$, where $\tilde{l}_k = f(l_k) =$

$f_{\text{sc}}(f_{\text{bl}}(f_{\text{clip}}(l_k)))$, i.e., $f \triangleq f_{\text{sc}} \circ f_{\text{bl}} \circ f_{\text{clip}}$ denotes the entire pre-processing. A natural mapping of quantized losses to bit vectors \mathbb{B}^q is assumed where quantization levels are mapped in ascending order to $(0, \dots, 0, 0)^\top$, $(0, \dots, 0, 1)^\top, \dots, (1, \dots, 1, 1)^\top$.

The transmitter (sink) has no knowledge of the functions $f_{\text{clip}}(\cdot)$, $f_{\text{bl}}(\cdot)$, or $f_{\text{sc}}(\cdot)$, and interprets the losses as being in the interval $[0, 1]$. It thus applies $\hat{l}_k = Q^{-1}(\tilde{l}_k) \in [0, 1]$ and uses the values \hat{l}_k in (4). We note that this approach is reminiscent of the POP-ART algorithm from [28], where rewards are shifted and scaled to enable learning across rewards with large dynamic range.

C. Impact of Feedback Quantization

The effect of quantization can be assessed via the Bussgang Theorem [29], which is a generalization of MMSE decomposition. If we assume $l_k \sim p(l)$ with mean μ_l and variance σ_l^2 , then

$$Q(l_k) = gl_k + w_k, \quad (8)$$

in which $g \in \mathbb{R}$ is the Bussgang gain and w_k is a random variable, uncorrelated with l_k , provided we set

$$g = \frac{\mathbb{E}\{l_k Q(l_k)\} - \mu_l \mathbb{E}\{Q(l_k)\}}{\sigma_l^2}. \quad (9)$$

When the number of quantization bits q increases, $Q(l_k) \rightarrow l_k$ and thus $g \rightarrow 1$.

If we replace l_k with $Q(l_k)$ in (5), denote the corresponding gradient function by $\nabla_\tau \ell_T^q(\tau)$, and substitute (8), then the following proposition holds.

Proposition 1. Let $\gamma_k = l_k \nabla_\tau \log \pi_\tau(\tilde{x}_k | m_k)$, $l_k \in [0, 1]$, with $\nabla_\tau \ell_T(\tau) = \mathbb{E}\{\gamma_k\}$, and $\gamma_k^q = Q(l_k) \nabla_\tau \log \pi_\tau(\tilde{x}_k | m_k)$, then

$$\mathbb{E}\{\gamma_k^q\} = \nabla_\tau \ell_T^q(\tau) = g \nabla_\tau \ell_T(\tau) \quad (10)$$

$$\mathbb{V}\{\gamma_k^q\} \leq g^2 \mathbb{V}\{\gamma_k\} + (g\bar{w} + \bar{w}^2) \text{tr}\{\mathbf{J}(\tau)\} \quad (11)$$

where $\mathbf{J}(\tau) = \mathbb{E}\{\nabla_\tau \log \pi_\tau(\tilde{x}_k | m_k) \nabla_\tau \log \pi_\tau(\tilde{x}_k | m_k)^\top\} \succeq 0$ is the Fisher information matrix of the transmitter parameters τ and $\bar{w} = \max_l |gl - Q(l)| = |1 - 1/2^{q-1} - g|$ is a measure of the maximum quantization error.

Proof: See Appendix. ■

Hence, the impact of quantization, under a sufficiently large mini-batch size is a scaling of the expected gradient. Note that this scaling will differ for each mini-batch. The variance is affected in two ways: a scaling with g^2 and an additive term that depends on the maximum quantization error and the Fisher information at τ . When q increases, $g \rightarrow 1$ and $\bar{w} \rightarrow 0$, so that $\mathbb{V}\{\gamma_k^q\} \rightarrow \mathbb{V}\{\gamma_k\}$, as expected.

In general, the value of g is hard to compute in closed form, but for 1-bit quantization and a Gaussian loss distribution, (9) admits a closed-form solution.⁴ In particular,

$$g = \begin{cases} 1/\sqrt{8\pi\sigma_l^2} & \mu_l = 1/2 \\ e^{-1/(8\sigma_l^2)}/\sqrt{8\pi\sigma_l^2} & \mu_l \in \{0, 1\}. \end{cases} \quad (12)$$

⁴For Gaussian losses, \bar{w} in Proposition 1 is not defined. The proposition can be modified to deal with unbounded losses.

In light of the distributions from Fig. 2, we observe that (after loss transformation) for most iterations, $\mu_l \approx 1/2$ and σ_l^2 will be moderate (around $1/(8\pi)$), leading to $g \approx 1$. Only after many iterations $\mu_l < 1/2$ and σ_l^2 will be small, leading to $g \ll 1$. Hence, for sufficiently large batch sizes, 1-bit quantization should not significantly affect the learning convergence rate.

D. Impact of Noisy Feedback Channels

For the proposed pre-processing and quantization scheme, distortions are introduced through the function $f(\cdot)$ (in particular the clipping) and the quantizer $Q(\cdot)$. Moreover, additional impairments may be introduced when the quantized losses are transmitted over a noisy feedback channel. We will consider the case where the feedback channel is a binary symmetric channel with flip probability $p \in [0, 1/2)$. Our numerical results (see Sec. V-B4) indicate that the learning process is robust against such distortions, even for very high flip probabilities. In order to explain this behavior, it is instructive to first consider the case where the transmitted per-sample losses are entirely random and completely unrelated to the training data. In that case, one finds that

$$\mathbb{E}\{\hat{l}_k \nabla_\tau \log \pi_\tau(\tilde{x}_k | m_k)\} = \mathbb{E}\{\hat{l}_k\} \mathbb{E}\{\nabla_\tau \log \pi_\tau(\tilde{x}_k | m_k)\} = 0$$

regardless of the loss distribution or quantization scheme. The interpretation is that for large mini-batch sizes, random losses simply “average out” and the applied gradient in (4) is close to zero. We can exploit this behavior and make the following statement.

Proposition 2. Let $\gamma_k^e = \hat{l}_k \nabla_\tau \log \pi_\tau(\tilde{x}_k | m_k)$ where the binary version of $Q(l_k)$ has been subjected to a binary symmetric channel with flip probability p to yield \hat{l}_k . Then, for 1-bit and 2-bit quantization, we have

$$\mathbb{E}\{\gamma_k^e\} = \nabla_\tau \ell_T^e(\tau) = (1 - 2p) \nabla_\tau \ell_T^q(\tau).$$

Moreover, for 1-bit quantization,

$$\mathbb{V}\{\gamma_k^e\} \leq \mathbb{V}\{\gamma_k^q\} + 4p(1 - p) \|\nabla_\tau \ell_T^q(\tau)\|^2 + p \text{tr}\{\mathbf{J}(\tau)\}.$$

Proof: See Appendix. ■

Hence, for a sufficiently large mini-batch size, the gradient is simply scaled by a factor $1 - 2p$. This means that even under very noisy feedback, learning should be possible.

Remark 2. Note that when using small mini-batches, the empirical gradients computed via (4) will deviate from the expected value $(1 - 2p) \nabla_\tau \ell_T^q(\tau)$: they will not be scaled exactly by $1 - 2p$ and they will be perturbed by the average value of $p \nabla_\tau \log \pi_\tau(\tilde{x}_k | m_k)$. Hence, robustness against large p can only be offered for large mini-batch sizes.

V. NUMERICAL RESULTS

In this section, we provide extensive numerical results to verify and illustrate the effectiveness of the proposed loss quantization scheme. In the following, the binary feedback channel is always assumed to be noiseless except for the results presented in Sec. V-B4.⁵

⁵TensorFlow source code is available at <https://github.com/henkwyneersch/quantizedfeedback>.

TABLE I: Neural network parameters, where $M = 16$

	transmitter f_τ			receiver f_ρ		
layer	1	2-3	4	1	2-3	4
number of neurons	M	30	2	2	50	M
activation function	-	ReLU	linear	-	ReLU	softmax

A. Setup and Parameters

1) *Channel Models*: We consider two memoryless channel models $p(y|x)$: the standard AWGN channel $y = x + n$, where $n \sim \mathcal{CN}(0, \sigma^2)$, and a nonlinear optical channel defined by the recursion

$$x_{i+1} = x_i e^{jL\gamma|x_i|^2/K} + n_{i+1}, \quad 0 \leq i < K, \quad (13)$$

where $x_0 = x$ is the channel input, $y = x_K$ is the channel output, $n_{i+1} \sim \mathcal{CN}(0, \sigma^2/K)$, L is the total link length, σ^2 is the noise power, and $\gamma \geq 0$ is the nonlinearity parameter.⁶ Note that the optical channel reverts to the AWGN channel when $\gamma = 0$. For our numerical analysis, we set $L = 2000$ km, $\gamma = 1.27$, $K = 20$, and $\sigma^2 = -21.3$ dBm. For both channels, we define $\text{SNR} \triangleq P/\sigma^2$.

2) *Transmitter and Receiver Networks*: Following previous work, the functions f_τ and f_ρ are implemented as multi-layer neural networks. A message m is first mapped to an M -dimensional "one-hot" vector where the m -th element is 1 and all other elements are 0. Each neuron takes inputs from the previous layer and generates an output according to a learned linear mapping followed by a fixed nonlinear activation function. The final two outputs of the transmitter network are normalized to ensure $1/B \sum_{k=1}^B |x_k|^2 = P$, $B \in \{B_T, B_R\}$, and then used as the channel input. The real and imaginary parts of the channel observation serve as the input to the receiver network. All network parameters are summarized in Table I, where $M = 16$.

3) *Training Procedure*: For the alternating optimization, we first fix the transmitter and train the receiver for $N_R = 30$ iterations with a mini-batch size of $B_R = 64$. Then, the receiver is fixed and the transmitter is trained for $N_T = 20$ iterations with $B_T = 64$. This procedure is repeated $N = 4000$ times. The Adam optimizer is used to perform the gradient updates, where $\alpha_T = 0.001$ and $\alpha_R = 0.008$.

4) *Transmitter Exploration Variance*: We found that the parameter σ_p^2 has to be carefully chosen to ensure successful training. In particular, choosing σ_p^2 too small will result in insufficient exploration and slow down the training process. On the other hand, if σ_p^2 is chosen too large, the resulting noise may in fact be larger than the actual channel noise, resulting in many falsely detected messages and unstable training. In our simulations, we use $\sigma_p^2 = P \cdot 10^{-3}$.

B. Results and Discussion

1) *Perfect vs Quantized Feedback*: We start by evaluating the impact of quantized feedback on the system performance, measured in terms of the symbol error rate (SER). For the

⁶This model is obtained from the nonlinear Schrödinger equation by neglecting dispersive effects. Analytical expressions for the PDF $p(y|x)$ can be found for example in [30].

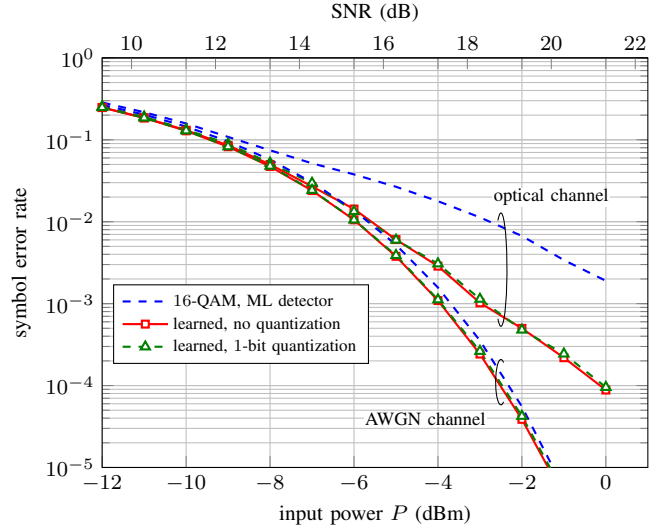


Fig. 3: Symbol error rate achieved for $M = 16$. The training SNR is 15 dB for the AWGN channel, whereas training is done separately for each input power (i.e., SNR) for the optical channel.

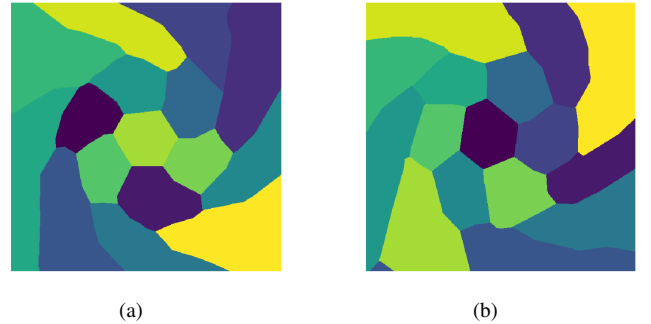


Fig. 4: Learned decision regions for the nonlinear optical channel, $M = 16$, and $P = -5$ dBm (a) without quantizing per-sample losses and (b) using the proposed quantization scheme and 1-bit quantization.

AWGN channel, the transmitter and receiver is trained for a fixed $\text{SNR} = 15$ dB (i.e., $P = -6.3$ dBm) and then evaluated over a range of SNRs (similar to, e.g., [12]). For the optical channel, this approach cannot be used because optimal signal constellations and receivers are highly dependent on the transmit power.⁷ Therefore, a separate transmitter–receiver pair is trained for each input power P . Fig. 3 shows the achieved SER assuming both perfect feedback without quantization and a 1-bit feedback signal based on the proposed method. For both channels, the resulting communication systems have very similar performance, indicating that the feedback quantization does not significantly effect the learning process. As a reference, the performance of standard 16-QAM with a maximum-likelihood (ML) detector is also shown. The learning approach outperforms this baseline for both channels.

Fig. 4 visualizes the learned decision regions for the quantized (right) and unquantized (left) feedback schemes assuming the optical channel with $P = -5$ dBm. Only slight differences are observed which can be largely attributed to the

⁷In principle, the optimal signal constellation may also depend on the SNR for the AWGN channel.

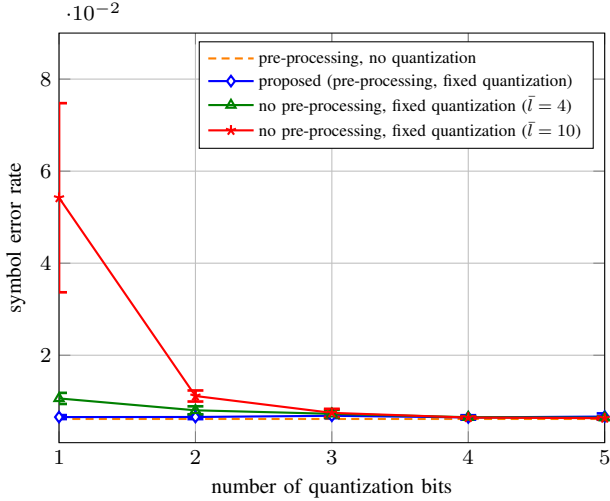


Fig. 5: Impact of the number of quantization bits on the achieved performance for the nonlinear optical channel with $M = 16$, $P = -5$ dBm. Results are averaged over 10 different training runs where error bars indicate the standard deviation between the runs.

randomness of the training process.

2) *Impact of Number of Quantization Bits:* Next, the optical channel for a fixed input power $P = -5$ dBm is considered to numerically evaluate the impact of the number of quantization bits on the performance. Fig. 5 shows the achieved SER when different schemes are used for quantizing the per-sample losses. For a fixed quantization scheme without pre-processing (see Sec. IV-A), the performance of the trained system is highly sensitive to the number of quantization bits and the assumed quantization range $[0, \bar{l}]$. For $\bar{l} = 10$ with 1 quantization bit, the system performance deteriorates noticeably and the training outcome becomes unstable, as indicated by the error bars (which are averaged over 10 different training runs). For the proposed quantization scheme, the performance of the trained system is (i) essentially independent on the number of bits used for quantization and (ii) virtually indistinguishable from a system trained with unquantized feedback.

3) *Impact on Convergence Rate:* In Fig. 6, we show the evolution of the empirical cross-entropy loss $\ell_T^c(\tau)$ during the alternating optimization for the optical channel with $P = -5$ dBm. It can be seen that quantization manifests itself primarily in terms of a slightly decreased convergence rate during training. For the scenario where per-sample losses are quantized with 5 bits, the empirical losses $\ell_T^c(\tau)$ converged after about 80 iterations, which is the same as in the case of unquantized feedback. For 1-bit quantization, the training converges slightly slower, after around 100 iterations.

4) *Impact of Noisy Feedback:* In order to numerically evaluate the effect of noise during the feedback transmission, we consider again the fiber optical channel for a fixed input power $P = -5$ dBm. Fig. 7 shows the achieved SER when transmitting the quantized per-sample losses over a binary symmetric channel with flip probability p (see Sec. IV-D). It can be seen that the proposed quantization scheme is highly robust to the channel noise. For the assumed mini-batch size $B_T = 64$, performance starts to decrease only for very high flip probabilities and remains essentially unchanged for

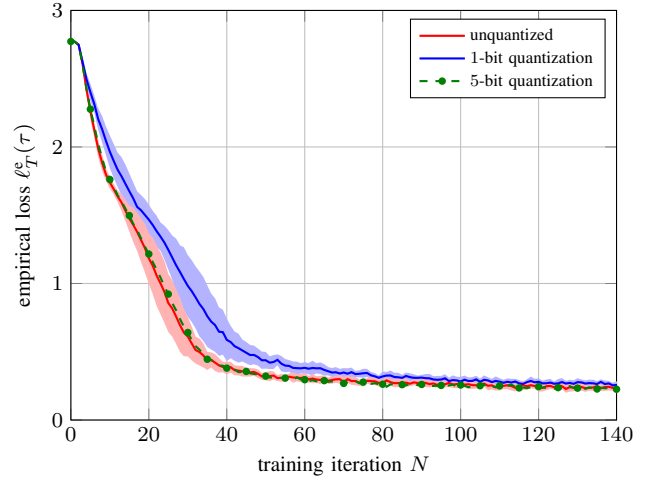


Fig. 6: Evolution of $\ell_T^c(\tau)$ during the alternating optimization for the fiber optical channel with $M = 16$, $P = -5$ dBm. Results are averaged over 15 different training runs where the shaded area indicates one standard deviation between the runs.

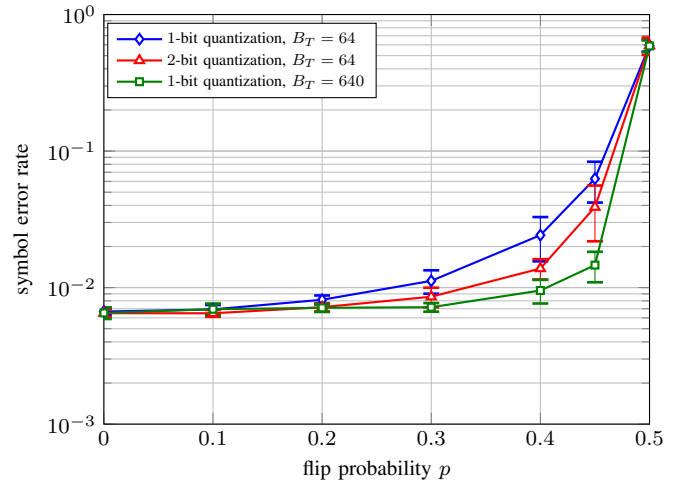


Fig. 7: Performance on fiber optical channel with $M = 16$, $P = -5$ dBm when transmitting quantized losses over a noisy feedback channel modeled as a binary symmetric channel with flip probability p . Results are average over 10 runs where the error bars indicate one standard deviation between runs.

$p < 0.1$ with 1-bit quantization and for $p < 0.2$ with 2-bit quantization. A theoretical justification for this behavior is provided in Proposition 2, which states that the channel noise manifests itself only as a scaling of the expected gradient. Thus, one may also expect that the learning process can withstand even higher flip probabilities by simply increasing the mini-batch size. Indeed, Fig. 7 shows that when increasing the mini-batch size from $B_T = 64$ to $B_T = 640$, the noise tolerance for 1-bit quantization increases significantly and performance remains unchanged for flip probabilities as high as $p = 0.3$.

Note that for $p = 0.5$, the achieved SER is slightly better than $(M - 1)/M \approx 0.938$ corresponding to random guessing. This is because the receiver learning is still active, even though the transmitter only performs random explorations.

VI. CONCLUSIONS

We have proposed a novel method for data-driven learning of physical-layer communication in the presence of a binary feedback channel. Our method relies on an adaptive clipping, shifting, and scaling of losses followed by a fixed quantization at the receiver, and a fixed reconstruction method at the transmitter. We have shown that the proposed method (i) can lead to good performance even under 1-bit feedback; (ii) does not significantly affect the convergence speed of learning; and (iii) is highly robust to noise in the feedback channel.

The proposed method can be applied beyond physical-layer communication, to reinforcement learning problems in general, and distributed multi-agent learning in particular.

APPENDIX

Proof of Proposition 1

The mean of γ_k^q can be computed as

$$\begin{aligned} \mathbb{E}\{\gamma_k^q\} &= \nabla_\tau \ell_T^q(\tau) \\ &= \mathbb{E}\{Q(l_k) \nabla_\tau \log \pi_\tau(\tilde{x}_k | m_k)\} \\ &= g \mathbb{E}\{l_k \nabla_\tau \log \pi_\tau(\tilde{x}_k | m_k)\} + \mathbb{E}\{w_k \nabla_\tau \log \pi_\tau(\tilde{x}_k | m_k)\} \\ &= g \mathbb{E}\{l_k \nabla_\tau \log \pi_\tau(\tilde{x}_k | m_k)\} + \mathbb{E}\{w_k\} \mathbb{E}\{\nabla_\tau \log \pi_\tau(\tilde{x}_k | m_k)\} \\ &= g \mathbb{E}\{l_k \nabla_\tau \log \pi_\tau(\tilde{x}_k | m_k)\} = g \nabla_\tau \ell_T(\tau). \end{aligned}$$

We have made use of the fact that w_k is uncorrelated with l_k and that (6) holds. The variance can similarly be bounded as follows:

$$\begin{aligned} \mathbb{V}\{\gamma_k^q\} &= \mathbb{E}\{(Q(l_k))^2 \|\nabla_\tau \log \pi_\tau(\tilde{x}_k | m_k)\|^2\} - g^2 \|\nabla_\tau \ell_T(\tau)\|^2 \\ &= g^2 \mathbb{E}\{l_k^2 \|\nabla \log \pi_\tau(x_k | m_k)\|^2\} - g^2 \|\nabla_\tau \ell_T(\tau)\|^2 \\ &\quad + \mathbb{E}\{w_k^2 \|\nabla \log \pi_\tau(x_k | m_k)\|^2\} \\ &\quad + 2 \mathbb{E}\{g l_k w_k \|\nabla \log \pi_\tau(x_k | m_k)\|^2\} \\ &\leq g^2 \mathbb{V}\{\gamma_k\} + \bar{w}^2 \text{tr}\{\mathbf{J}(\tau)\} \\ &\quad - 2g \mathbb{E}\{w_k l_k \|\nabla \log \pi_\tau(\tilde{x}_k | m_k)\|^2\} \\ &\leq g^2 \mathbb{V}\{\gamma_k\} + \bar{w}^2 \text{tr}\{\mathbf{J}(\tau)\} + 2g \bar{w} \text{tr}\{\mathbf{J}(\tau)\} \end{aligned}$$

We have made use of $-w_k l_k = l_k(g l_k - Q(l_k)) \leq \max_{l_k} |g l_k - Q(l_k)| = \bar{w}$, that $l_k \leq 1$, and that $\text{tr}\{\mathbf{J}(\tau)\} = \mathbb{E}\{\|\nabla \log \pi_\tau(x_k | m_k)\|^2\}$.

Proof of Proposition 2

For the proposed adaptive pre-processing and fixed 1-bit quantization, the quantized losses l_k are either $\Delta/2 = 1/4$ or $1 - \Delta/2 = 3/4$. Assuming transmission over the binary symmetric channel, the gradient in (5) can be written as

$$\nabla_\tau \ell_T^e(\tau) = \mathbb{E}\{Q(l_k)^{1-n_k} (1 - Q(l_k))^{n_k} \nabla_\tau \log \pi_\tau(\tilde{x}_k | m_k)\},$$

where n_k are independent and identically distributed Bernoulli random variables with parameter p . Since n_k is independent of all other random variables, we can compute

$$\mathbb{E}[Q(l_k)^{1-n_k} (1 - Q(l_k))^{n_k} | Q(l_k)] = (1 - 2p)Q(l_k) + p.$$

Hence,

$$\begin{aligned} \mathbb{E}\{\gamma_k^e\} &= \nabla_\tau \ell_T^e(\tau) \\ &= \mathbb{E}\{((1 - 2p)Q(l_k) + p) \nabla_\tau \log \pi_\tau(\tilde{x}_k | m_k)\} \\ &= (1 - 2p) \mathbb{E}\{Q(l_k) \nabla_\tau \log \pi_\tau(\tilde{x}_k | m_k)\} + p \mathbb{E}\{\nabla_\tau \log \pi_\tau(\tilde{x}_k | m_k)\} \\ &= (1 - 2p) \nabla_\tau \ell_T^q(\tau), \end{aligned}$$

where the last step follows from (6). For 2-bit quantization, the possible values are $\Delta/2 = 1/8$ (corresponding to bits 00), $3\Delta/2 = 3/8$ (corresponding to 01), $1 - 3\Delta/2 = 5/8$ (corresponding to 10), $1 - \Delta/2 = 7/8$ (corresponding to 11). It then follows that when the transmitted loss is $Q(l_k)$, the received loss is

$$\begin{aligned} &Q(l_k) \text{ with prob. } (1 - p)^2 \\ &1 - Q(l_k) \text{ with prob. } p^2 \\ &\text{other with prob. } p(1 - p) \end{aligned}$$

so that the expected received loss is $(1 - 2p)Q(l_k) + p$.

The variance under 1-bit quantization can be computed as

$$\begin{aligned} \mathbb{V}\{\gamma_k^e\} &= \mathbb{E}\{(\gamma_k^e)^2\} - (1 - 2p)^2 \|\nabla_\tau \ell_T^q(\tau)\|^2 \\ &= \mathbb{E}\{(Q(l_k))^{2(1-n_k)} (1 - Q(l_k))^{2n_k} \|\nabla_\tau \log \pi_\tau(\tilde{x}_k | m_k)\|^2\} \\ &\quad - (1 - 2p)^2 \|\nabla_\tau \ell_T^q(\tau)\|^2 \\ &= \mathbb{E}\{Q^2(l_k) \|\nabla_\tau \log \pi_\tau(\tilde{x}_k | m_k)\|^2\} + p \mathbb{E}\{\|\nabla \log \pi_\tau(\tilde{x}_k | m_k)\|^2\} \\ &\quad - 2p \mathbb{E}\{Q(l_k) \|\nabla \log \pi_\tau(\tilde{x}_k | m_k)\|^2\} - (1 - 2p)^2 \|\nabla_\tau \ell_T^q(\tau)\|^2 \\ &= \mathbb{V}\{\gamma_k^q\} + 4p(1 - p) \|\nabla_\tau \ell_T^q(\tau)\|^2 + p \text{tr}\{\mathbf{J}(\tau)\} \\ &\quad - 2p \mathbb{E}\{Q(l_k) \|\nabla_\tau \log \pi_\tau(\tilde{x}_k | m_k)\|^2\} \\ &\leq \mathbb{V}\{\gamma_k^q\} + 4p(1 - p) \|\nabla_\tau \ell_T^q(\tau)\|^2 + p \text{tr}\{\mathbf{J}(\tau)\}, \end{aligned}$$

where the last step holds since $Q(l_k) \geq 0$.

REFERENCES

- [1] N. Samuel, T. Diskin, and A. Wiesel, "Deep MIMO Detection," in *Proc. IEEE Int. Workshop on Signal Processing Advances in Wireless Communications (SPAWC)*, 2017.
- [2] E. Nachmani, E. Marciano, L. Lugosch, W. J. Gross, D. Burshtein, and Y. Be'ery, "Deep Learning Methods for Improved Decoding of Linear Codes," *IEEE J. Sel. Topics Signal Proc.*, vol. 12, no. 1, pp. 119–131, Feb. 2018.
- [3] T. O'Shea and J. Hoydis, "An Introduction to Deep Learning for the Physical Layer," *IEEE Trans. on Cognitive Communications and Networking*, vol. 3, no. 4, pp. 563–575, Dec. 2017.
- [4] S. Dörner, S. Cammerer, J. Hoydis, and S. ten Brink, "Deep Learning-Based Communication Over the Air," *IEEE J. Sel. Topics Signal Proc.*, vol. 12, no. 1, pp. 132–143, Feb. 2017.
- [5] B. Karanov, M. Chagnon, F. Thouin, T. A. Eriksson, H. Bülow, D. Lavery, P. Bayvel, and L. Schmalen, "End-to-end deep learning of optical fiber communications," *J. Lightw. Technol.*, vol. 36, no. 20, pp. 4843–4855, 2018.
- [6] S. Li, C. Häger, N. Garcia, and H. Wymeersch, "Achievable information rates for nonlinear fiber communication via end-to-end autoencoder learning," in *Proc. European Conf. Optical Communication (ECOC)*, Rome, Italy, 2018.
- [7] R. T. Jones, T. A. Eriksson, M. P. Yankov, and D. Zibar, "Deep Learning of Geometric Constellation Shaping including Fiber Nonlinearities," in *Proc. European Conf. Optical Communication (ECOC)*, Rome, Italy, 2018.
- [8] H. Lee, I. Lee, and S. H. Lee, "Deep learning based transceiver design for multi-colored VLC systems," *Opt. Express*, vol. 26, no. 5, pp. 6222–6238, Mar. 2018.
- [9] T. J. O'Shea, T. Roy, and N. West, "Approximating the Void: Learning Stochastic Channel Models from Observation with Variational Generative Adversarial Networks," *arXiv:1805.06350*, 2018.

- [10] H. Ye, G. Y. Li, B.-H. F. Juang, and K. Sivasenan, "Channel Agnostic End-to-End Learning based Communication Systems with Conditional GAN," *arXiv:1807.00447*, 2018.
- [11] F. A. Aoudia and J. Hoydis, "End-to-End Learning of Communications Systems Without a Channel Model," *arXiv:1804.02276*, 2018.
- [12] —, "Model-free Training of End-to-end Communication Systems," *arXiv:1812.05929*, 2018.
- [13] C. de Vrieze, S. Barratt, D. Tsai, and A. Sahai, "Cooperative Multi-Agent Reinforcement Learning for Low-Level Wireless Communication," *arXiv:1801.04541*, 2018.
- [14] V. Raj and S. Kalyani, "Backpropagating Through the Air: Deep Learning at Physical Layer Without Channel Models," *IEEE Commun. Lett.*, vol. 22, no. 11, pp. 2278–2281, Nov. 2018.
- [15] M. Goutay, F. A. Aoudia, and J. Hoydis, "Deep Reinforcement Learning Autoencoder with Noisy Feedback," *arXiv:1810.05419*, 2018.
- [16] M. Kim, W. Lee, J. Yoon, and O. Jo, "Building Encoder and Decoder with Deep Neural Networks: On the Way to Reality," *arXiv:1808.02401*, 2018.
- [17] Z.-L. Tang, S.-M. Li, and L.-J. Yu, "Implementation of Deep Learning-based Automatic Modulation Classifier on FPGA SDR Platform," *Electronics*, vol. 7, no. 7, p. 122, 2018.
- [18] C.-F. Teng, C.-H. Wu, K.-S. Ho, and A.-Y. Wu, "Low-complexity Recurrent Neural Network-based Polar Decoder with Weight Quantization Mechanism," *arXiv:1810.12154*, 2018.
- [19] C. Fougstedt, C. Häger, L. Svensson, H. D. Pfister, and P. Larsson-Edefors, "ASIC Implementation of Time-Domain Digital Backpropagation with Deep-Learned Chromatic Dispersion Filters," in *Proc. European Conf. Optical Communication (ECOC)*, Rome, Italy, 2018.
- [20] F. A. Aoudia and J. Hoydis, "Towards Hardware Implementation of Neural Network-based Communication Algorithms," *arXiv:1902.06939*, 2019.
- [21] A. Y. Ng, D. Harada, and S. J. Russell, "Policy invariance under reward transformations: Theory and application to reward shaping," in *Proceedings of the Sixteenth International Conference on Machine Learning*. Morgan Kaufmann Publishers Inc., 1999, pp. 278–287.
- [22] V. Mnih, K. Kavukcuoglu, D. Silver, A. A. Rusu, J. Veness, M. G. Bellemare, A. Graves, M. Riedmiller, A. K. Fidjeland, G. Ostrovski *et al.*, "Human-level control through deep reinforcement learning," *Nature*, vol. 518, no. 7540, p. 529, 2015.
- [23] R. S. Sutton and A. G. Barto, *Reinforcement learning: An introduction*. MIT press, 2018.
- [24] D. P. Kingma and J. Ba, "Adam: A Method for Stochastic Optimization," in *Proc. ICLR*, 2015.
- [25] S. Gu, T. Lillicrap, Z. Ghahramani, R. E. Turner, and S. Levine, "Q-prop: Sample-efficient policy gradient with an off-policy critic," *arXiv preprint arXiv:1611.02247*, 2016.
- [26] R. Islam, P. Henderson, M. Gomrokchi, and D. Precup, "Reproducibility of benchmarked deep reinforcement learning tasks for continuous control," *arXiv preprint arXiv:1708.04133*, 2017.
- [27] S. Lloyd, "Least squares quantization in pcm," *IEEE transactions on information theory*, vol. 28, no. 2, pp. 129–137, 1982.
- [28] H. P. van Hasselt, A. Guez, M. Hessel, V. Mnih, and D. Silver, "Learning values across many orders of magnitude," in *Advances in Neural Information Processing Systems*, 2016, pp. 4287–4295.
- [29] H. Rowe, "Memoryless nonlinearities with Gaussian inputs: Elementary results," *The BELL system technical Journal*, vol. 61, no. 7, pp. 1519–1525, 1982.
- [30] K. S. Turitsyn, S. A. Derevyanko, I. V. Yurkevich, and S. K. Turitsyn, "Information Capacity of Optical Fiber Channels with Zero Average Dispersion," vol. 91, no. 20, p. 203901, nov 2003.